Coherent control of Bloch oscillations by means of optical pulse shaping

R. Fanciulli* and A. M. Weiner
Physics Department and School of Electrical and Computer Engineering, Purdue University, West Lafayette, Indiana 47907, USA

M. M. Dignam
Physics Department, Queen's University, Kingston, Ontario, Canada K7L 3N6

D. Meinhold and K. Leo
Institut für Angewandte Photophysik, Technische Univerität Dresden, D-010609 Dresden, Germany
(Received 11 October 2004; published 12 April 2005)

We excite excitonic wave packets in biased semiconductor superlattices with spectrally shaped ultrashort optical pulses. We tailor the shape and phase of the pulse spectrum in order to control the coherent dynamics of the excitonic wave packets formed from a superposition of three excitonic states. Via careful shaping, we are able to excite either wave packets that exhibit standard Bloch oscillations (BO's) or breathing-mode (BM) motion. These two types of motion are characterized by the presence (BO) or absence (BM) of an internal intraband polarization caused by the electron-hole separation within the excitonic wave packet. The wave packet evolution is monitored using spectrally resolved four-wave mixing. This ability to control the BO's provides a way to control the emitted THz radiation.

DOI: 10.1103/PhysRevB.71.153304 PACS number(s): 78.47.+p, 42.65.Re, 78.67.Pt

Although periodic oscillations of a charge carrier in a periodic potential with a uniform applied electric field were predicted many years ago,[1] scattering effects prevented their observation until semiconductor superlattices (SL's) were employed.[2] Over roughly the last decade, several groups have used femtosecond optical excitation to initiate such Bloch oscillations (BO's) in semiconductor SL's, which are then observed through a variety of techniques such as degenerate four-wave mixing (DFWM), THz spectroscopy, and electro-optic sampling.[3] BO's have also been observed in different systems such as Bose-Einstein condensates in optical lattices.[4] In this paper, for the first time to our knowledge, we apply coherent control (CC) techniques to manipulate these wave packet dynamics. By doing so we have achieved coherent THz oscillations of the macroscopic electric-dipole moment lasting over several oscillation periods, which can be switched on and off according to pulse shape. Techniques of CC,[5] in which specially shaped ultrafast laser pulses[6] are used to manipulate quantum mechanical processes, have been applied to many systems. Examples include control of photochemical reactions,[7] energy flow in photosynthetic molecules,[8] chemically selective photoexcitation,[9] and selective enhancement of high-harmonic radiation.[10] Such experiments are characterized by complex laser wave forms selected through stochastic learning algorithms. In contrast, CC experiments in semiconductors typically involve very simple laser wave forms, such as pulse doublets. For example, interference between contributions from the individual pulses led to enhancement or suppression of exciton generation in a single quantum well[11] and of wave packet amplitude in a double quantum well.[12] A similar technique has also been applied for control of tipping angle in spin ensembles.[13] In contrast, our experiments in a semiconductor SL utilize a more complex laser wave form and result in wave packets made up primarily of three basis states, whose individual amplitudes and phases are manipulated under pulse-shape control. This yields the ability to switch between breathing mode and Bloch oscillation wave packet types, a degree of control that goes well beyond earlier semiconductor CC experiments. Our excitation scheme can be used to optimize the THz output, which is important for possible tunable THz emitter devices.

We use a $GaAs/Al_{0.3}Ga_{0.7}As$ SL composed of 35 quantum wells (67 Å/17 Å),[3] which is etched to be used in a transmission geometry and is cooled down to 10 K. Applying an external dc bias F_{bias} breaks the translational symmetry of the SL and breaks the minibands into equally spaced electronic levels, forming the Wannier-Stark ladder (WSL). In a noninteracting electron picture, the energies of the electronic states are given by

$$E_n = E_0 + neF_{bias}d, \tag{1}$$

where e is the elementary charge, d is the spatial period of the SL, and n is the number of the well the electron is excited to (relative to its initial well).

The wave functions corresponding to these levels are localized and roughly centered in each well.[14] A study of the interband oscillator strengths[15] allows us to consider only the transitions from the heavy hole to the lowest level in each well in the conduction band (1*S* excitonic levels). For the field strengths considered here, we can label each transition unequivocally in terms of the WSL well number n (see Fig. 1). The effect of a broadband laser pump pulse on our system is to excite each electron into a superposition of these states. Due to the uniform energy spacing of the WSL ($eF_{bias}d$) and the spatial localization of the corresponding electronic wave functions, the excitonic wave packet will oscillate spatially among the quantum wells whose levels were covered by the laser spectrum. The period of this intraband oscillation is given by $T_{BO}=h/eF_{bias}d$.

We use a transform-limited, 50-fs [fullwidth at half maxi-

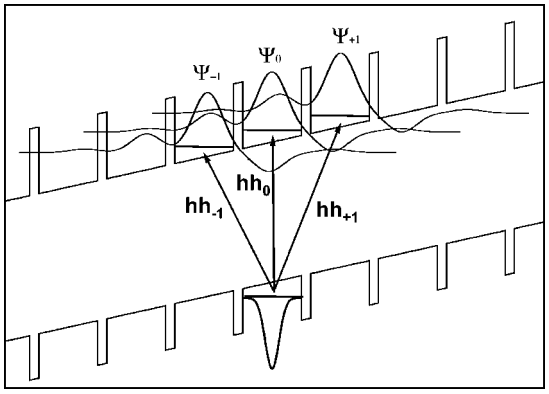

FIG. 1. Representation of the superlattice. A schematic of the electronic wave functions and the transitions of interest in our experiment are reported.

mum (FWHM) bandwidth of 31 meV] pulse from a Ti:S laser centered at 1.594 eV. In order to control the electron dynamics with our laser pulses, we make use of a Fourier-transform pulse shaper[6] that allows us to apply at the same time amplitude and phase modulations to the spectrum of our pump pulses. In order to observe the BO, we perform spectrally resolved DFWM (SR-DFWM). By measuring the spectrum of the $2\vec{k}_2-\vec{k}_1$ signal ($\vec{k}_1$ being the wave vector of the pump and $\vec{k}_2$ that of the probe) as a function of the delay τ between pulses 2 and 1, we can observe the signature of the intraband BO in the interband polarization induced by the laser pulses. Each transition covered by the laser gives a separate component in the DFWM spectrum which can be studied separately. In our experiments we tuned the laser center wavelength and bandwidth to excite the three excitonic transitions: hh_0, hh_{+1}, and hh_{-1}. Due to the electron-hole interaction, the excitonic WSL levels are not quite equally spaced. However, many features of the results can be understood via the following simple, single-electron picture.[15] Defining $\Psi_n(x)$ as the electronic wave function centered in the nth well, the pump pulse creates the superposition of three states given by

$$\Psi(x) = A_{-1}e^{+i\omega_{BO}t}\Psi_{-1}(x) + A_0\Psi_0(x) + A_{+1}e^{-i\omega_{BO}t}\Psi_{+1}(x). \tag{2}$$

Here, A_n is a complex number proportional to the product of S_n and M_n, where S_n is the laser complex spectral amplitude resonant with the nth transition and M_n is the interband dipole matrix element. Due to the alternating sign of the WSL wave function on the high-energy side (see Fig. 1), M_{-1} and M_{+1} have opposite signs.[15] If we now consider only overlap integrals between nearest-neighbor wells, the expectation value for the position of the excited single electron is given by

$$\begin{aligned} X_e(t) = (&|A_{-1}|^2x_{-1} + |A_0|^2x_0 + |A_{+1}|^2x_{+1}) - 2|A^*_{-1}A_0| \\ &\times|x_{-1,0}|\cos(\omega_{BO}t + \phi_{-1}) + 2|A^*_{+1}A_0||x_{+1,0}|\cos(\omega_{BO}t \\ &+ \phi_{+1}), \end{aligned} \tag{3}$$

where ϕ_n is the phase of S_n, $x_{n,m} \equiv \int_{-\infty}^{+\infty}\Psi^*_n(x)x\Psi_m(x)dx$, and $x_n \equiv x_{n,m}\delta_{n,m}$. To a good approximation, $x_{-1,0}$ and $x_{+1,0}$ are equal and opposite.[15] According to Eq. (3), by manipulating the phase and amplitude of the $A_{\pm1}$, the dynamics of the center of mass of the electron can be controlled to display an oscillatory behavior (BO's) or nonoscillatory behavior [breathing mode (BM)]. An experiment aimed at the observation of the BM and BO was reported previously.[16] To make the oscillations symmetric and obtain a BM, the spectrum of the pump was shifted in order to change the relative values of A_{+1} and A_{-1}. Although inherently simple, this approach displayed a few limitations. The parameter A_0 that appears in Eqs. (2) and (3) could not be separately controlled. The temporal window in which the oscillations could be clearly observed was limited with only half a BO period being reported. On the other hand, in our experiment, through amplitude modulation, we excite predominantly 1S excitons and control the parameters A_n separately. This creates a kicked-oscillator type of dynamics that prolongs the coherence, allowing the observation of up to six oscillations over a window of more than 1.5 ps. Moreover, by adjusting the phases $\phi_{\pm1}$, we are able to switch between BM and BO modes and control the initial direction of oscillation of the BO mode. This demonstrates our ability to generate tunable and well-controlled THz oscillatory dynamics with long temporal coherence. Due to the strong localization of the hole in its initial well, caused by its larger effective mass, we can define an oscillating intraband polarization approximately as $P_{int}(t) = -Ne[X_e(t) - x_{hole}]$, where N is the excitation density. If we consider the ensemble of all the oscillating excitons, this macroscopic, oscillating, intraband polarization will yield an internal time-varying (ac) field that will alternatively screen and reinforce the external field F_{bias}. The effect of this internal field is to shift the excitonic energies. As Lyssenko *et al.*[17] have shown, it is possible to monitor the internal motion of excitons by observing the effect of this internal dipole on the transitions energy. We will, therefore, take advantage of this mechanism to monitor the effects of our control over the excitonic dynamics. Creating the same number of excitons in the hh_{+1} and hh_{-1} states, we can make the magnitude of the two parameters A_{-1} and A_{+1} of Eqs. (2) and (3) identical. From Eq. (3), if the relative phase between S_{-1} and S_{+1} is zero, this has the effect of creating the symmetric wave packet motion that maintains the center of mass of the electron fixed in the well of origin at all times (BM). In order to achieve the breathing mode, we carefully choose the pump spectrum to account for the different dipole matrix elements of the hh_{-1} and hh_{+1} transitions. This can be seen in Fig. 2 where both the absorption spectrum of the SL (at the V_{bias} of choice) and the spectrum of the pump and probe pulses are plotted. In Fig. 3 we can see that our optical spectrum corresponds to a train of pulses in time. This train of pulses acts in a similar way to the periodic driving force of a classical oscillator. However, in our case the main (fastest) dampening effect is not provided by a loss of energy, but by a dephasing and decoherence of the oscillators within the excited ensemble. With each pulse in the train, we compensate for any loss in the coherence by adding new excitons in phase with the existing ensemble. This effect is visible in the inset of Fig. 3 where the ratio between the height of the peaks of the temporal profile of the FWM (hh_{-1} transition only) and the

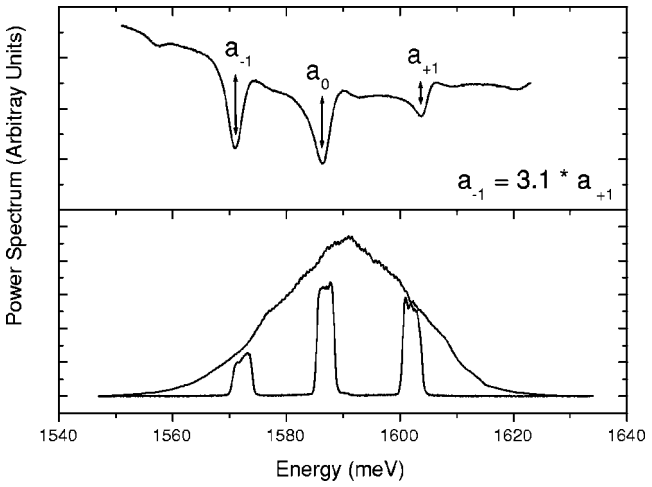

FIG. 2. (a) Absorption spectrum of the SL for $V_{bias}=1.3$ V. (b) Spectra of the unshaped (probe) and shaped (pump) laser pulses.

cross correlation is reported versus peak number. Note that the last peak in the FWM temporal profile is entirely due to wave packet dynamics. The effect of such an excitation (with constant phase profile $[\phi_{-1},\phi_0,\phi_{+1}]=[0,0,0]$ for the three spectral components) over the electronic dynamics is reported in Fig. 4(a) where the position of the hh_{-1} transition is reported as a function of the delay τ. Within the sensitivity of our experiments, no clearly oscillating variation in the peak position is observed. This is because the oscillating internal intraband polarization P_{int} that acts to screen the bias field is very small due to the symmetry of the BM. In Fig. 3 we showed through the interband polarization (FWM) the presence of BO dynamics, while in Fig. 4(a) we show the suppression of the intraband dipole. This clearly demonstrates the quite different physics represented by the two types of polarization. From Eq. (3), we see that adding a $\pm\pi$ phase

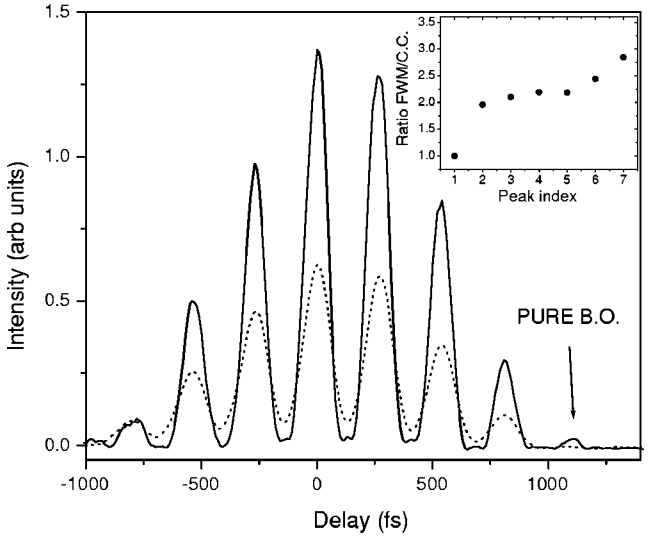

FIG. 3. Solid line: height of the hh_{-1} component of the DFWM spectrum versus time. Dotted line: cross correlation (CC) of the pump pulse. The excitation spectrum has a flat phase [0,0,0]. Inset: ratio of the peaks heights of DFWM and CC versus peak number (for increasing delays).

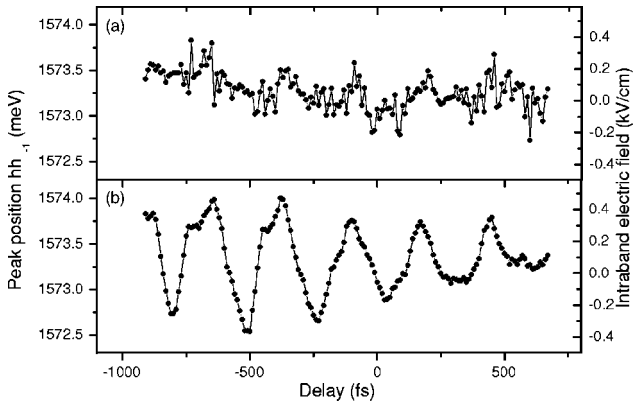

FIG. 4. Peak position of the hh_{-1} in the case of the (a) nonbreathing mode (phase of the pump pulse $[\pi,0,0]$) and (b) breathing mode (phase of the pump pulse [0,0,0]). The right scale reports the estimated magnitude of the generated internal oscillatory THz field as estimated using the quasistatic model.

shift to either S_{+1} or S_{-1} destroys the symmetry of the breathing mode and creates a BO mode of maximum amplitude. In Fig. 4(b) we report the oscillations of the peak position of the hh_{-1} transition when a phase profile $[\pi,0,0]$ is applied to the pump spectrum (see Fig. 2). The difference between the breathing and nonbreathing mode cases (Fig. 4) appears rather striking. In the breathing mode the electronic wave packet expands and contracts over time symmetrically with respect to the central well. This is verified, within experimental error, in our data by the lack of oscillation in the transition energies (and therefore of internal oscillating dipole). When we apply an asymmetric phase shift to the pump spectrum, we induce an asymmetry in the excitonic dynamics and we lead the system out of the BM regime and into the BO one. This is verified by the presence of clear oscillatory behavior in the energy position of the transitions.

The understanding of the detailed dynamics and nonlinear interactions is rather complicated. A theory of the dynamics of 1*S* excitonic wave packets valid to infinite order in the optical field has been developed.[18] As this theory does not account for continuum states, it is not accurate in the current situation. However, it is possible to estimate the effect of the intraband polarization on the transitions positions positions with a simple quasistatic picture. Using a maximum amplitude of oscillation of one SL period, our excitation density of about 5×10^9 electrons/pulse/well/cm^2, the measured linear dependence of the $hh_{\pm1}$ transitions on the applied field [1.75 meV/(kV/cm)], and an average value for the dielectric constant of the two materials of $12.8\epsilon_0$, the expected peak shift is of about 0.4 meV. As can be verified in Fig. 4, this result is in reasonably good agreement with our data.

As a last step we want to use the parallel between the spatial phase of the electronic oscillator and the optical phase in our pump spectrum. We show how by adjusting the relative phase of the $A_{\pm1}$ parameters, we can control the direction of motion of the excited electrons. By applying a phase to the side peaks of the pump spectrum, we are effectively controlling the parameters $\phi_{\pm1}$ of Eq. (3). An example is reported in Fig. 5. In this case, in the first scan a $[\phi_{-1},\phi_0,\phi_{+1}]=[0,0,\pi]$ phase profile was applied. In the

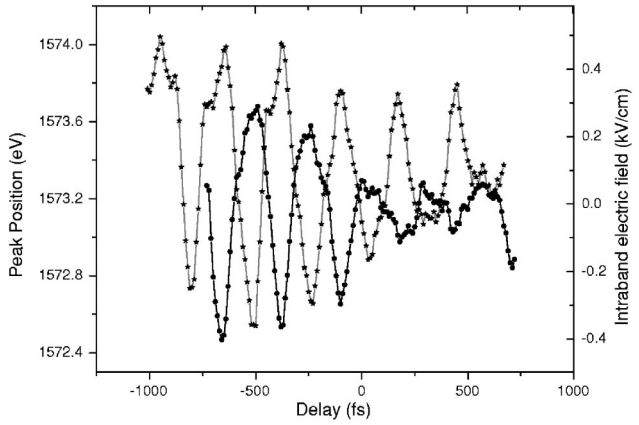

FIG. 5. Effect of the coherent control. Dots: a phase of $[\pi,0,0]$ is applied to the pump spectrum. Stars: a phase of $[0,0,\pi]$ is applied to the pump spectrum. The right scale reports the estimated magnitude of the generated internal oscillatory THz field as estimated using the quasistatic model.

next scan the situation was reversed, with the π phase applied to the hh_{-1} ($[\pi,0,0]$). The π phase shift observed in the plot of the energy of the hh_{-1} versus time can be viewed as the result of the change of the initial direction of motion of the electrons.

We have demonstrated full control over the coherent electronic dynamics. We first created breathing modes by purely amplitude modulating the pump pulse. Then we adjusted the phases of each spectral component of the pump pulse to generate nonbreathing modes with macroscopic time-varying internal electric dipole moment and finally to control completely the electronic dynamics. The results are qualitatively explained in terms of a simple quasistatic model. We are currently developing a full theory of the coherent nonlinear dynamics of the 1*S* and continuum excitonic states.

We have shown the possibility of controlling the THz time scale internal dynamics of oscillating excitons. One could perform similar experiments in this system in which shaped pulses are used to switch on or off the THz radiation associated with BO.

We wish to acknowledge K. Köhler of the Fraunhofer Institut in Freiburg for providing the SL structures. The work of MMD was supported in part by the Natural Sciences and Engineering Research Council of Canada.

*Electronic address: riccardo@physics.purdue.edu

[1] F. Bloch, Z. Phys. **52**, 555 (1928).
[2] L. Esaki and R. Tsu, IBM J. Res. Dev. **14**, 61 (1970).
[3] K. Leo, *High-Field Transport in Semiconductor Superlattices* (Springer-Verlag, Berlin, 2003).
[4] O. Morsch, J. H. Mller, M. Cristiani, D. Ciampini, and E. Arimondo, Phys. Rev. Lett. **87**, 140402 (2001).
[5] H. Rabitz, R. D. Vivie-Riedle, and K. K. M. Motzkus, Science **288**, 824 (2000).
[6] A. Weiner, Rev. Sci. Instrum. **71**, 1929 (2000).
[7] R. Levis, G. Menkir, and H. Rabitz, Science **292**, 709 (2001).
[8] J. Herek, W. Wohlleben, R. Cogdell, D. Zeidler, and M. Motzkus, Nature (London) **417**, 6888 (2002).
[9] T. Brixner, N. Damrauer, P. Niklaus, and G. Gerber, Nature (London) **414**, 57 (2001).
[10] R. Bartels, S. Backus, E. Zeek, L. Misoguti, G. Vdovin, I. Christov, M. Murnane, and H. Kapteyn, Nature (London) **406**, 164 (2000).
[11] A. Heberle, J. J. Baumberg, and K. Kohler, Phys. Rev. Lett. **75**, 2598 (1995).
[12] P. Planken, I. Brener, M. Nuss, M. Luo, and S. Chuang, Phys. Rev. B **48**, 4903 (1993).
[13] J. Gupta, R. Knobel, N. Samarth, and D. Awschalom, Science **292**, 2458 (2001).
[14] A. Bouchard and M. Luban, Phys. Rev. B **52**, 5105 (1995).
[15] M. Dignam, J. Sipe, and J. Shah, Phys. Rev. B **49**, 10502 (1994).
[16] M. Sudzius, V. Lyssenko, F. Löser, K. Leo, M. Dignam, and K. Köhler, Phys. Rev. B **57**, R12693 (1998).
[17] V. Lyssenko, G. Valusis, F. Löser, T. Hasche, K. Leo, M. Dignam, and K. Köhler, Phys. Rev. Lett. **79**, 301 (1997).
[18] M. Hawton and M. Dignam, Phys. Rev. Lett. **91**, 267401 (2003).